International Journal of Research in Engineering, Science and Management
Volume 4, Issue 3, March 2021
https://www.ijresm.com | ISSN (Online): 2581-5792

Creep Behaviour of 316 Austenitic Stainless Steel at Elevated Temperatures

P. Arunachalam[1], K. Srimuralidharan[2*], N. Satheesh Kumar[3], K. Sriram[4], G. Saran Raj[5]
[1,2,3,4,5]*Department of Mechanical Engineering, Sri Eshwar College of Engineering, Coimbatore, India*

***Abstract*: Austenitic stainless steels are used for domestic, industrial, transport, and architectural products based primarily on their corrosion resistance but also for their formability, their strength, and their properties at extreme temperatures. We conducted a creep test of two different specimen of same material at 550 °C/275 MPa and 650 °C/225 MPa. During creep test a specimen 2 tested at 650 °C/225 MPa rupture faster when comparing with specimen 1 tested at 550 °C/275 MPa. Even though specimen 1possess high stress value when comparing with specimen 2 rupture life is high due to temperature lower than specimen 2. This shows temperature is dependent factor for creep testing of materials. Microstructure of two specimens are after testing show similar microstructure after creep. Residual cells were still observable in limited areas in both specimens. Variations in the high stress specimen are highly dependent on grain orientations. The residual dislocation cell structure observed in the 316 SS creep specimens may be understood by the dependence of dislocation substructure on grain orientation. creep specimens may be understood by the dependence of dislocation substructure on grain orientation dislocation cell structure observed in the 316 SS.**

***Keywords*: Creep, Microstructure, 316 Austenitic stainless steel.**

1. Introduction

Creep is defined as the progressive deformation at a constant stress. It occurs below the yield strength of the material when it is exposed for long time to a high level of stress (Fig. 1). Creep is also more severe to those materials which are subjected to heat for long periods, close to melting point. Creep perpetually increases with increase in temperature. The rate of this deformation is a function of the material properties, exposure time, exposure temperature and also the applied structural load. Depending on the magnitude of the applied stress and its duration, the deformation might become so large that a component can no longer perform its function - for example creep of a turbine blade will cause the blade to contact the casing, resulting in the failure of the blade. Creep is sometimes of concern to engineers and metallurgists when determining components that are operating under high stresses or high temperatures. Creep is a deformation mechanism that may or may not constitute a failure mode. Sometimes moderate creep in concrete is welcomed as a result of it relieves tensile stresses which may otherwise lead to cracking. In contrast to brittle fracture, creep failure doesn't occur suddenly upon the application of stress. Instead, strain accumulates as a result of long-term stress .Creep can be defined as time-dependent deformation at absolute temperatures greater than one half the absolute melting. This relative temperature (*T* (*abs*)/*Tmp* (*abs*)) is known as the homologous temperature. Several examples illustrate this point.

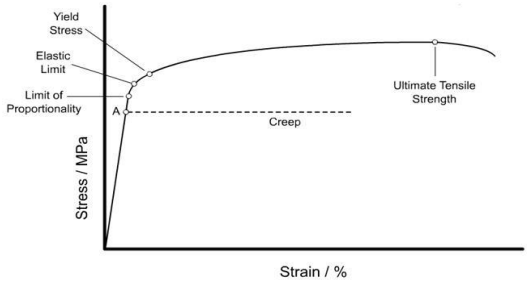

Fig. 1. Stress –strain diagram showing creep below the yield strength of the material due to long exposure to high levels of stress

2. Material Selection

A. 316 Austenitic Stainless Steels

316 is a chromium-nickel-molybdenum austenitic stainless steel with good strength and excellent corrosion resistance, as supplied in the annealed condition with a typical Brinell hardness of 175. Characterized by high corrosion resistance in marine and industrial atmospheres, it exhibits excellent resistance to chloride attack and against complex sulphur compounds employed in the pulp and paper processing industries. The addition of 2% to 3% of molybdenum increases its resistance to pitting corrosion and improves its creep resistance at elevated temperatures. Also it displays good oxidation resistance at elevated temperatures and has excellent weldability.316 cannot be hardened by thermal treatment, but strength and hardness can be increased substantially by cold working, with subsequent reduction in ductility. It is now available with improved machinability (by calcium injection treatment), which has little effect on corrosion resistance and weldability while greatly increasing feeds and/or speeds, plus extending tool life. It is used extensively by the Marine, Chemical, Petrochemical, Pulp and Paper, Textile, Transport, Manufacturing and allied industries.

*Corresponding author: srimuralidharan67@gmail.com

B. Specimen Preparation

Specimens are prepared as per the ASTM standard by using Wire cut EDM.

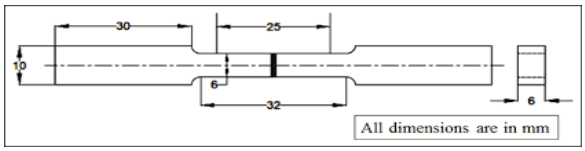

Fig. 2. ASTM standard for specimen

Wire cut EDM (or WCEDM) discharges the electrified current by means of a taut thin wire, which acts as the cathode and is guided alongside the desired cutting path, or kerf. The dielectric fluid in this case—usually deionized water is flushed through the cut as it proceeds, again serving to carry off particles and control the sparks. The thin wire allows precision cuts, with narrow kerfs (~0.015 in. routinely, with finer kerfs available) and tolerances of +/- 0.0001 in. possible. This heightened precision allows for complex, three-dimensional cuts, and produces highly accurate punches, dies, and stripper plates.

3. Creep Testing

In a conventional creep test, the specimen is loaded to constant stress and temperature. The main purpose of performing the creep test is to determine the maximum stress and temperature up to which the material can sustain for a long time. That is, evaluating the creep resistance of the material and the resultant plastic deformation (strain) is measured and plotted as a function of time. For brittle materials, creep tests are conducted under compression loading, where the specimens used are right cylinders with an aspect ratio (length to diameter) ranging from 2 to 4. Creep tests can be performed at a given temperature at different stresses or at different temperatures for a given stress level. Eventually, all data are collected to obtain the creep behaviour of the material. Figure 3 shows the experimental setup of a creep tester with specimen loading.

Fig. 3. Experimental setup of a creep tester

Hold a specimen at a constant elevated temperature under a fixed applied stress and observe the strain produced. Test that extend beyond 10% of the life expectancy of the material in service are preferred. Mark the sample in two locations for a length dimension. Apply a load. Measure the marks over a time period and record deformation.

4. Microstructure Evaluation by SEM

The scanning electron microscope (SEM) uses a focused beam of high-energy electrons to generate a variety of signals at the surface of solid specimens. The signals that derive from electron-sample interactions reveal information about the sample including external morphology (texture), chemical composition, and crystalline structure and orientation of materials making up the sample. In most applications, data are collected over a selected area of the surface of the sample, and a 2-dimensional image is generated that displays spatial variations in these properties. Areas ranging from approximately 1 cm to 5 microns in width can be imaged in a scanning mode using conventional SEM techniques (magnification ranging from 20X to approximately 30,000X, spatial resolution of 50 to 100 nm).

Fig. 4. Scanning electron microscope setup

5. Result and Analysis

A. Creep Analysis

Table 1
Experimental result

Sample	Time (seconds)	Time (hrs)	Strain
Material 1	23400	6.50	0.07
Material 2	18800	5.22	0.08

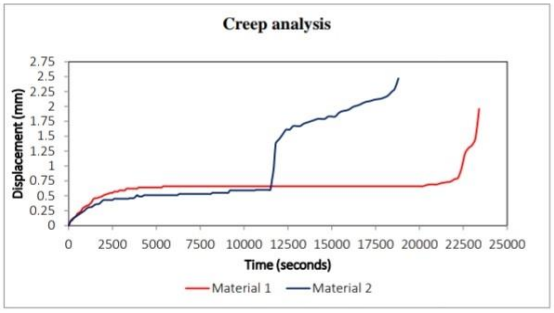

Fig. 5. Creep curve obtained after creep testing

B. Microstructure Analysis

The microstructure of the as-built 316 SS was examined by SEM. For SEM examination, a small portion is cut off from the 316 austenitic stainless steel plate. During scanning it produce images of a sample by scanning the surface with a focused beam of electron. SEM images at various magnifications in Fig. 6, reveal well-organized dislocation cell structure with the mean cell size of 530 nm. The dislocation density is low inside the

cells. Minimal misorientations were observed between dislocation substructures, cell walls consisted of dislocation tangles, and substructures were considered as dislocation cells. Elemental segregation was observed at cell boundaries which were enriched in Cr and Mo and depleted of Fe. Microstructure of the creep-tested specimens was also examined by SEM. SEM disk specimens of 3 mm in diameter were cut from the gauge section of a specimen away from the fracture surface of the creep-tested specimen. Fig. 7, (a and b) shows the microstructure of as-built 316 SS after creep test at 550°C/275 MPa and 650°C/225 MPa, respectively. It was found that the initial dislocation cell structure in the as-built 316 SS gradually disappeared during creep and evolved into a uniformly-distributed high-density dislocation structure. Two 316 SS specimens tested in different creep conditions, 550°C/275 MPa and 650°C/225 MPa, show similar microstructure after creep. Residual cells were still observable in limited areas in both specimens. Kestenbach et al. [11] showed that dislocation structure varies considerably among individual grains of the same specimen under creep. Variations in the high stress specimen are highly dependent on grain orientations. The residual dislocation cell structure observed in the 316 SS creep specimens may be understood by the dependence of dislocation substructure on grain orientation. It was also observed that the residual dislocation cells in the creep-tested specimens were smaller than the dislocation cells in the as-built specimen (530 nm). A mean size of 382 nm was measured in the 650°C/225 MPa specimen, and 334 nm in the 550°C/275 MPa in the limited areas studied under SEM

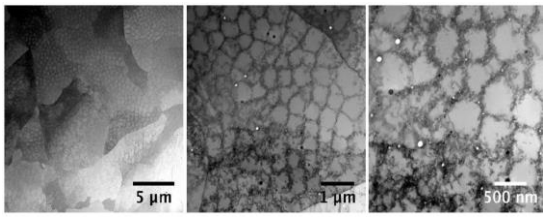

Fig. 6. Microstructure of 316 stainless steel before creep testing by SEM at different magnification

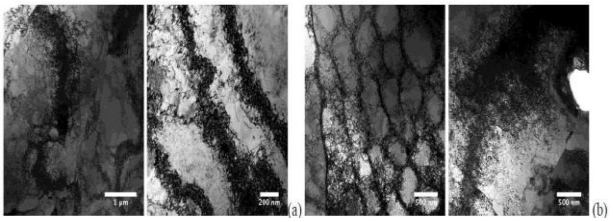

Fig. 7. Microstructure of 316 austenitic stainless steel at a) 550°C/275MPa, b) 650°C/225MPa

C. Effect of Heat Treatment on Creep Behaviour of 316 SS

To evaluate the effect of post-build heat treatments on the creep behavior of 316 SS, the heat-treated specimens were tested under the same condition, 550 °C and 275 MPa, and their creep curves are compared. The 650 °C-heat treated specimens have longer creep lives than the specimens in the as-built and all other heat-treated conditions. All the specimens show similar creep response, exhibiting predominantly accelerated creep. Fig. 8, 9, 10, plot the creep rupture time, the minimum creep rate, and the creep elongation as a function of heat treatment temperature, respectively. The creep rupture time of 316 SS reached the maximum after the heat treatment at 650 °C, then decreased continuously with increasing heat treatment temperature, and reached the minimum at 900 °C. The 1050 °C heat treatment slightly restored the creep rupture life. The minimum creep rate followed the opposite trend and reached the minimum after the heat treatment at 650 °C and the maximum at 900 °C. It is interesting to note that the 650 °C-heat treated specimens showed the lowest creep elongations, but the longest creep lives.

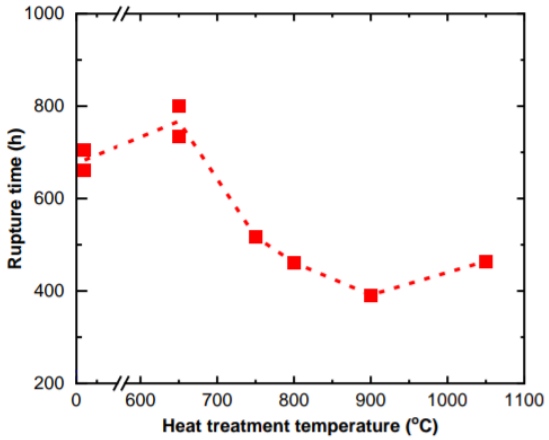

Fig. 8. Effect of heat treatments on the creep rupture life of 316 SS tested at 550 °C 275 MPa

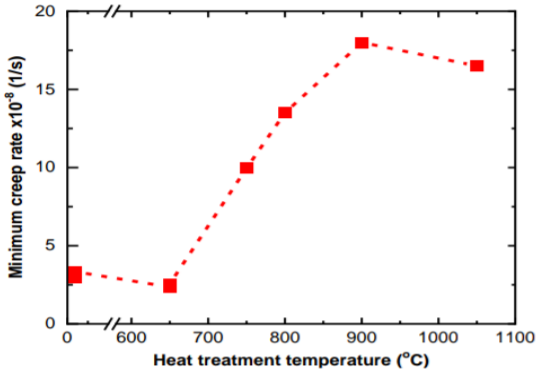

Fig. 9. Effect of heat treatments on the minimum creep strain rate of 316 SS tested at 550°C 275 MPa

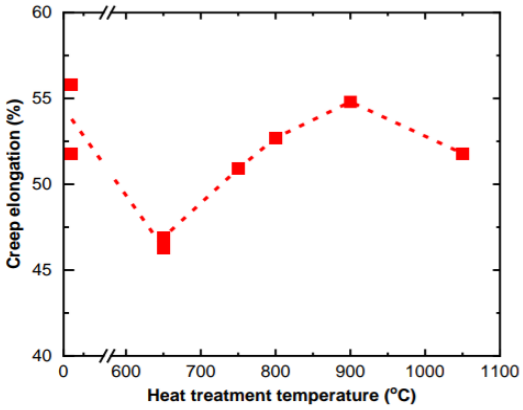

Fig. 10. Effect of heat treatments on the creep elongation of 316 SS tested at 550 °C 275 MPa

6. Conclusion

We conducted a creep test of two different specimen of same material at 550 °C/275 MPa and 650 °C/225 MPa. During creep test a specimen 2 tested at 650°C/225 MPa rupture faster when comparing with specimen 1 tested at 550 °C/275 MPa. Even though specimen 1 possess high stress value when comparing with specimen 2 rupture life is high due to temperature lower than specimen 2. This shows temperature is dependent factor for creep testing of materials. Microstructure of two specimens are after testing show similar microstructure after creep. Residual cells were still observable in limited areas in both specimens. Variations in the high stress specimen are highly dependent on grain orientations. The residual dislocation cell structure observed in the 316 SS creep specimens may be understood by the dependence of dislocation substructure on grain orientation.

References

[1] J. He, R. Sandström, Basic modelling of creep rupture in austenitic stainless steels, Theoretical and Applied Fracture Mechanics, 2017.

[2] Song Xue Tao and Yang Ruidong, "Crack analysis of Cr-Mo-V-Si medium-carbon alloy steel in casting die Author links open overlay panel," 2020.

[3] S. Ravi, P. Parameswaran, J. Ganeshkumar, S. Sakthy, K. Laha, "Failure analysis of 316L austenitic stainless steel bellows used under dynamic sodium in a creep testing chamber," Engineering Failure Analysis, vol. 59, pp. 366-376, 2016.

[4] Martinez-Ubeda, A. I., Griffiths, I., Karunaratne, M. S. A., Flewitt, P. E. J., Younes, C., & Scott, T. (2016). Influence of nominal composition variation on phase evolution and creep life of Type 316H austenitic stainless steel components: 21st European Conference on Fracture, ECF21, 20-24 June 2016, Catania, Italy. 958-965.

[5] Babak Shalchi Amirkhiz, Su Xu, Colin Scott, "Microstructural assessment of 310S stainless steel during creep at 800 °C," Materialia, vol. 6, 100330, 2019.

[6] J. Hu, G. Green, S. Hogg, R. Higginson, A.C.F. Cocks, Effect of Microstructure evolution on the creep properties of a polycrystalline 316H austenitic stainless steel, Materials Science & Engineering; A, 2020.

[7] Punit Kumar, A.K. Mondal, S.G. Chowdhury, G. Krishna, Ashok Kumar Ray, "Influence of additions of Sb and/or Sr on microstructure and tensile creep behaviour of squeeze-cast AZ91D Mg alloy," Materials Science and Engineering: A, vol. 683, pp. 37-45, 2017.

[8] Deepshree D. Awale, V. D. Vijayanand, Atul R. Ballal, Manjusha M. Thawre, J. Ganesh Kumar, G.V. Prasad Reddy, "Evaluation of tensile properties of various regions of creep exposed dissimilar weld joint using miniature specimen testing," Engineering Failure Analysis, vol. 120, 105079, 2021.

[9] Guocai Chai, Magnus Boström, Magnus Olaison and Urban Forsberg, Creep and LCF Behaviors of Newly Developed Advanced Heat Resistant Austenitic Stainless Steel for A-USC, 2013, Procedia Engineering, (55), 232-239.

[10] Richard J. Williams, Jalal Al-Lami, Paul A. Hooper, Minh-Son Pham, Catrin M. Davies, "Creep deformation and failure properties of 316 L stainless steel manufactured by laser powder bed fusion under multiaxial loading conditions," Additive Manufacturing, vol. 37, 101706, 2021.

[11] H. J. Kestenbach, T.L. Da Silveira, S.N. Monteiro, "On subgrain formation during creep pf 316 stainless steel," Metall. Trans. 7A (1976) 155.

[12] H. Cottrell. Theory of brittle fracture in steel and similar metals. Trans. AIME, 212:191–203, 1961.

[13] J. A. Williams. A theoretical dreivation of the creep life of commercial metals failing by triple point cracking. Phil. Mag., 15:1289–1291, 1967.

[14] H. E. Evans. The growth of creep cavities by grain boundary sliding. Phil Mag., 23(185):1101– 1112, 1971.

[15] D. A. Miller and T. G. Langdon. Creep fracture maps for 316 stainless steel. Metall. mater. trans., 10A:1635–1641, 1979.

[16] H. J. Frost and M. F. Ashby. Deformation mechanism maps. Pergamon press, Oxford, 1982.

[17] T. J. Chuang, K. T. Kagawa, and J. R. Rice. The shape of intergranular creep cracks groing by surface diffusion. Acta metall., 21:1625–1628, 1973.

[18] T. J. Chuang, K. T. Kagawa, J. R. Rice, and L. B. Sills. Non-equilibrium models for diffusive cavitation of grain interfaces. Acta metall, 27:265–284, 1979.

[19] C. F. Cocks and M. F. Ashby. On creep fracture by void growth. Prog. mater. sci., 27(3– 4):189–244, 1982.

[20] P. M. Anderson and J. R. Rice. Constrained creep cavitation of grain boundary facets. Acta metall., 33(3):409–422, 1985.

[21] V. Tvergaard. On the creep constrained diffusive cavitation of grain boundary facets. J. Mech. Phys. Solids, 32(5):373–393, 1984. Hales, R., 1983,

[22] R. Hales, "A Method of Creep Damage Summation Based on Accumulated Strain for the Assessment of Creep-Fatigue Endurance," Journal of Fatigue of Engineering Materials and Structures, 6, 121-135.

[23] Ohno, N., Wang, J, D., 1993, Kinematic Hardening Rules with Critical State of Dynamic Recovery, Part I: Formulation and Basic Features for Rachetting Behavior, International Journal of Plasticity, 9, 375-390

[24] Ohno, N., Abdel-Karim, M. and Kobayashi, M., 1998, Ratchetting Characteristics of 316FR Steel at High Temperature, Part I: Strain-Controlled Ratchetting experiments and simulations, International Journal of Plasticity, 14, 355-372

[25] Ohno, N., Yamamoto, R., Sasaki, T. and Okumura, D., 2017, Resetting scheme for Plastic Strain Surface in Constitutive Modeling of Cyclic Plasticity, ZAMM - Journal of Applied Mathematics and Mechanics, 98, 518-531

[26] Ohno, N., Sasaki, T., Shimada, T., Tokuda, K., Yoshida, K. and Okumura, D., 2018, Effect of Cyclic Hardening on Stress Relaxation in SUS316HTP Under Creep-Fatigue Loading at 700°C: Experiments and Simulations, Journal of Theoretical and Applied Mechanics, 56, 497- 510

[27] Priest, R, H. and Ellison, E, G., 1981, A Combined Deformation Map-Ductility Exhaustion Approach to Creep-Farigue Analysis., Journal of materials Science and Engineering, 49, 7-17.

[28] RCC-MR, Design and Construction Rules for mechanical Components of FBR Nuclear Islands, 2002, AFCEN, Paris.

[29] Wen, J, F., Tu, S, T., Xuan, F, Z., Zhang, X, W. and Gao, X, L., "Effects of Stress Level and Stress State on Creep Ductility: Evaluation of Different Models," Journal of Materials Science and Technology, 32, 695-704, 2016.